# Periodic stick-slip mode of ice surface premelting during friction

Alexei Khomenko<sup>a,b,\*</sup>, Denis Logvinenko<sup>a</sup>

<sup>a</sup>Department of Applied Mathematics and Complex Systems Modeling, Sumy State University, 40007 Sumy, Ukraine

## Abstract

The rheological nonlinear model of ice surface softening during friction is developed. Analytical and numerical schemes describing stick-slip frictional oscillations for three boundary relations between the shear strain, stress, and temperature relaxation times are built. The phase portraits and time dependencies of friction force are calculated. The random force (additive uncorrelated noise) effect on found damped oscillation mode is revealed. It is shown that white noise influence leads to an undamped oscillation mode corresponding to a periodic intermittent (stick-slip) regime of friction that is basically responsible for destruction of rubbing surfaces. The most pronounced such oscillatory behavior occurs if relaxation time of the temperature is much longer that its value for shear strain and stress.

Keywords: Ice surface softening, Viscoelastic medium, Friction force, Fluctuations intensity, Phase portraits, Stick-slip friction

<sup>&</sup>lt;sup>b</sup>Peter Grünberg Institut-1, Forschungszentrum-Jülich, D-52425 Jülich, Germany

<sup>\*</sup>Corresponding author. Sumy State University, 40007 Sumy, Ukraine. Tel.:  $38\ 0542\ 333155$ ; Fax:  $38\ 0542\ 334058$ .

Email address: o.khomenko@mss.sumdu.edu.ua (Alexei Khomenko) URL: personal.sumdu.edu.ua/khomenko/en/ (Alexei Khomenko)

#### 1. Introduction

The description of stick-slip mode of ice friction is widely approved as a result of transitions between two dynamic states during the stationary sliding due to presence of rapidly fluctuating (in space and time) domains of crystalline ice and liquid-like ice [1, 2, 3, 4, 5, 6, 7, 8, 9, 10, 11, 12]. The study of this mode has the fundamental significance for tribology, and also it can be used for prediction of friction reducing or increasing and liquidation of the negative influence of the interrupted mode of ice friction.

During ice friction three ranges of sliding speeds are distinguished, which are determined by such processes [1, 9, 10, 13]. The expression and estimation were obtained for low velocity at which the frictional energy dissipation initiates diminutive heating of the ice, and its melting does not take place. The slow logarithmic increase in the static rubbing occurs with the time of steady-state contact owing to, particularly, a slow ascent of the contact area. Besides, a logarithmic growth of the kinetic friction force takes place as a result of thermally activated creep [9]. The expression and estimation were found for high speed at which a thin continuous water film is generated on the sliding boundary owing to melting of ice conditioned by the frictional heat. The rubbing force is fixed by viscosity and thickness of water film, which are defined by the joint effect of ice surface melting and squeezing-out of formed water [13]. According to the B. Persson's theory of contact mechanics [1, 13], in the intermediate speed interval frictional heating changes friction due to thermal and shear premelting of the surface or the formation

of a heterogeneous thin surface layer. Based on one of these assumptions, it is possible to explain the variation of ice friction with growth of motion speed before its value, at which a thin homogeneous water film appears on the surface.

Some nonlinear models of boundary friction under conditions far from thermodynamic equilibrium have been developed [14, 15, 16]. These models allowed us to describe self-organization of different low-dimensional systems [17, 18]. At the same time, these methods were not applied to ice friction. Therefore, we developed the theory that allowed us to study the ice softening taking into account additive noncorrelated fluctuations of the shear strain and stress, and the temperature usually observed in reality [10, 11, 12]. We constructed the phase diagrams with different modes of friction showing that noise leads to the complication of ice premelting in the usual and self-similar modes.

Experimental data and calculations [1, 2, 3, 4, 5, 6, 7, 8, 9, 10, 11, 12] have shown that intermittent friction can be a stochastic regime in which the static and kinetic friction forces change randomly over time. However, stick-slip mode is also periodic in nature [2, 3, 7, 8]. The investigated in this paper stochastic model, which describes the oscillatory softening of ice surface during friction, will help to clarify the causes of this mode and its peculiarities.

The rheological model suggested in [10, 11, 12] for representation of ice friction is based on a system of dimensionless equations:

$$\tau_{\varepsilon}\dot{\varepsilon} = -\varepsilon + \sigma,\tag{1}$$

$$\tau_{\sigma}\dot{\sigma} = -\sigma + g(T-1)\varepsilon,\tag{2}$$

$$\tau_T \dot{T} = (T_e - T) - \sigma \varepsilon, \tag{3}$$

where  $\varepsilon$  is the shear component of strains which appear in the ice surface layer,  $\sigma$  is the shear component of stresses, and T is the ice surface temperature,  $\tau_{\varepsilon,\sigma,T}$  are relaxation times of corresponding quantities. Here, the constant  $g \equiv G_0/G_{\varepsilon} < 1$  is introduced, which is the ratio of the typical value  $G_0$  of shear modulus of ice to its relaxed value  $G_{\varepsilon}$ , and  $T_e$  is the thermostat temperature (temperature far away from rubbing surfaces). It was revealed that zero stationary strains  $\varepsilon_0$  meet the usual crystalline ice; at  $\varepsilon_0 \neq 0$  the ice softens.

In a steady state all derivatives in Eqs. (1)–(3) equal zero and the parameters of the ice stay constant with time. Analysis of the equations set shows that if background temperature  $T_e$  of rubbing blocks does not exceed the critical value

$$T_{c0} = 1 + g^{-1} (4)$$

shear strains take on stationary magnitude  $\varepsilon_0 = 0$ , while for  $T_e > T_{c0}$ , the value

$$\varepsilon_0 = \left[ T_e - \left( 1 + g^{-1} \right) \right]^{1/2},\tag{5}$$

meeting the premelting mode of friction, is realized.

According to proposed approach the softened ice film represents a strongly viscous liquid that can behave itself similar to the solid: has a high effective viscosity and still exhibits a yield stress [1, 4, 13]. The crystalline ice state corresponds to the shear strain  $\varepsilon = 0$  because the Kelvin-Voigt equation (1), containing the viscous stress, falls out of consideration. Maxwell-type equation (2) reduces to the Debye law describing the rapid relaxation of the

shear stress during the microscopic time  $\tau_{\sigma} = b/c \sim 10^{-12}$  s, where  $b \sim 1$  nm is the lattice constant or the intermolecular distance and  $c \sim 10^3$  m/s is the sound velocity [7, 8, 12]. Correspondingly the heat conductivity equation (3) assumes the form of simplest expression for temperature relaxation that does not contain the terms describing the dissipative heating and the mechanicand-caloric effect inherent in a viscous liquid. Basic equations (1)–(3) specify the above characteristics of the ice softened state at  $\varepsilon \neq 0$ . It is supposed that the frictional force decreases with the temperature growth owing to the weakening of hydrogen couplings between ice molecules. Moreover, the rubbing force descents with velocity increase at the contact  $v = l\partial\varepsilon/\partial t$ , because friction heat is generated and, therefore, a softened layer thickness l grows [1, 4, 13, 12].

The kinetics of setting the stationary state is strongly defined by the ratio of relaxation times [14, 15, 19]. Therefore the effect of different limiting ratios of these times will be examined further.

## 2. Periodic intermittent mode

## 2.1. The case $\tau_T \ll \tau_{\varepsilon}, \tau_{\sigma}$

Setting  $\tau_T \dot{T} \approx 0$  in Eq. (3), we express T from this equation and arrive at the two-parameter system (1), (2) plugging T into Eq. (2). Then, two resultant first-order differential equations in strain  $\varepsilon$  and stress  $\sigma$  can be reduced to a second-order equation in terms of  $\varepsilon$ . To this end, we should express  $\sigma$  in  $\varepsilon$  from Eq. (1) and take the time derivative of this relationship. Plugging these dependencies  $\sigma(\varepsilon,\dot{\varepsilon})$  and  $\dot{\sigma}(\dot{\varepsilon},\ddot{\varepsilon})$  into Eq. (2), we arrive at the sought equation. If time is measured in the units of  $\tau_{\varepsilon}$ , this equation can

be written in the form

$$\ddot{\varepsilon} + \frac{1 + \tau + g\varepsilon^2}{\tau} \dot{\varepsilon} + \frac{\varepsilon}{\tau} \left[ 1 + g\varepsilon^2 - g(T_e - 1) \right] = \xi(t), \tag{6}$$

where  $\tau = \tau_{\sigma}/\tau_{\varepsilon}$ . In Eq. (6) the random force  $\xi(t)$  is introduced additionally whose moments are defined by

$$\langle \xi_i(t) \rangle = 0, \quad \langle \xi_i(t)\xi_i(t') \rangle = 2D\delta_{ij}\delta(t - t'),$$
 (7)

where D acts as the intensity of Langevin source,  $\delta_{ij}$  is Kronecker delta symbol and  $\delta(t)$  stands for Dirac delta function. The reason for consideration of additive noise is the description of stick-slip friction mode by the simplest manner. The introduction of fluctuations in previous studies [10, 11] has allowed us to obtain the phase diagrams.

The canonical form of Eq. (6) is as follows

$$\ddot{\varepsilon} + 2\alpha\dot{\varepsilon} + \omega_0^2 \varepsilon = \xi(t), \tag{8}$$

where damping constant  $\alpha$  and natural frequency  $\omega_0$  of oscillations are strain dependent. The constant value of strains ( $\dot{\varepsilon} = 0$ ) is realized in the steady state (D = 0), therefore Eq. (5) can be obtained by setting the last term in the left-hand side of Eq. (6) to be equal to zero. The damping constant near the stationary point  $\varepsilon_0$  can easily be derived from Eq. (6). The value (5) when substituted into Eq. (6) yields relationship whose comparison with Eq. (8) gives sought damping constant:

$$\alpha = 0.5 \left[ 1 + g\tau^{-1}(T_e - 1) \right]. \tag{9}$$

In order to specify the character of oscillatory mode, we ought to determine  $\omega_0$  and frequency of damped oscillations  $\omega = \sqrt{\omega_0^2 - \alpha^2}$ . An example of

analysis of similar set of equations by phase plane method can be found in [19] and is planed in the future work.

For numerical solving Eq. (8), we can introduce the designation  $x = \dot{\varepsilon}$  that transforms the single second-order equation (8) into two first-order ones

$$\dot{\varepsilon} = x,$$

$$\dot{x} = -2\alpha x - \omega_0^2 \varepsilon + \xi(t). \tag{10}$$

The explicit expressions for  $\alpha$  and  $\omega_0$  are got from comparison of Eqs. (6) and (8). The equations system in the form of (10) is typical for study by phase plane method [19, 20, 21, 22]. The Euler method and following iterative procedure are used further for integration [10, 11, 14, 15]:

$$\varepsilon_2 = \varepsilon_1 + x_1 \triangle t,$$

$$x_2 = x_1 + (-2\alpha x_1 - \omega_0^2 \varepsilon_1) \triangle t + \sqrt{\triangle t} W_n.$$
(11)

To simulate stochastic force  $W_n$ , we employ the Box-Muller generator [23],

$$W_n = \sqrt{2D}\sqrt{-2\ln r_1}\cos(2\pi r_2), \quad r_i \in (0, 1], \tag{12}$$

where  $r_{1,2}$  are pseudorandom numbers with uniform distributions.

The phase portrait in Fig. 1a displays the result of numerical solution of Eq. (6) based on (11) and (12). The dotted isoclinal on which  $\dot{\varepsilon} = 0$  indicates the points at which the phase trajectories have a vertical tangent. The isoclinal line represents the abscissa axis within considered coordinates. The dot-and-dash isoclinal ( $\ddot{\varepsilon} = 0$ ) demonstrates the points at which the phase trajectories have a horizontal tangent. The relationship to build this isoclinal  $\dot{\varepsilon}(\varepsilon)$  is obtained from Eq. (6). It is apparent that phase portrait is

marked by the presence of three singular points: saddle point I at the origin, that is an unstable one since it meets the maximum of the synergetic potential [19, 24], and two points (nodes) S and S' which are symmetrically situated relatively to  $\varepsilon = 0$ . In the vicinity of the latter points a tendency towards an oscillatory mode manifests itself during establishment of steady state  $\varepsilon_0$ . However, this tendency is not realized in full due to the large value of the damping constant. For the given relationship between the relaxation times, the regime of rapidly damped oscillations is observed under both conditions  $\tau_{\varepsilon} \ll \tau_{\sigma}$  and  $\tau_{\varepsilon} \gg \tau_{\sigma}$  [19]. It is worth noting that positive and negative values of strains meet the movement of the top rubbing block in opposite directions. Particularly, according to the phase portrait the motion is possible in two directions for the positive (negative) initial values of  $\varepsilon = \sigma/G_{\varepsilon}$  and negative (positive) shear rate  $\dot{\varepsilon} = \sigma/\eta_{\varepsilon}$ . In the latter formula  $\sigma$  is the viscous (nonequilibrium) shear stress and  $\eta_{\varepsilon}$  is the effective shear viscosity that is characteristic of ultrathin "liquid" films confined between solid surfaces [14, 15, 16, 24].

Figure 2a depicts the time dependencies of friction force F corresponding to the trajectories in Fig. 1a. Figures 2a–c and 3a–c are built using approximation  $F(t) = AG_{\varepsilon}\varepsilon(t)$  as stated in Refs. [10, 11] (A is the contact area of rubbing surfaces). The total strain  $\varepsilon$  involves the elastic (equilibrium) component  $\varepsilon_{el}$  and the viscous (nonequilibrium) component  $\varepsilon_v$  which accordingly give contributions in the static and kinetic components of total friction force F. The dependencies in Fig. 2a illustrate an aperiodic transient stick-slip mode, i.e., during characteristical slip time force F relaxes to establishment of sliding at a constant shear rate ( $\dot{\varepsilon} = \text{const}$ ).

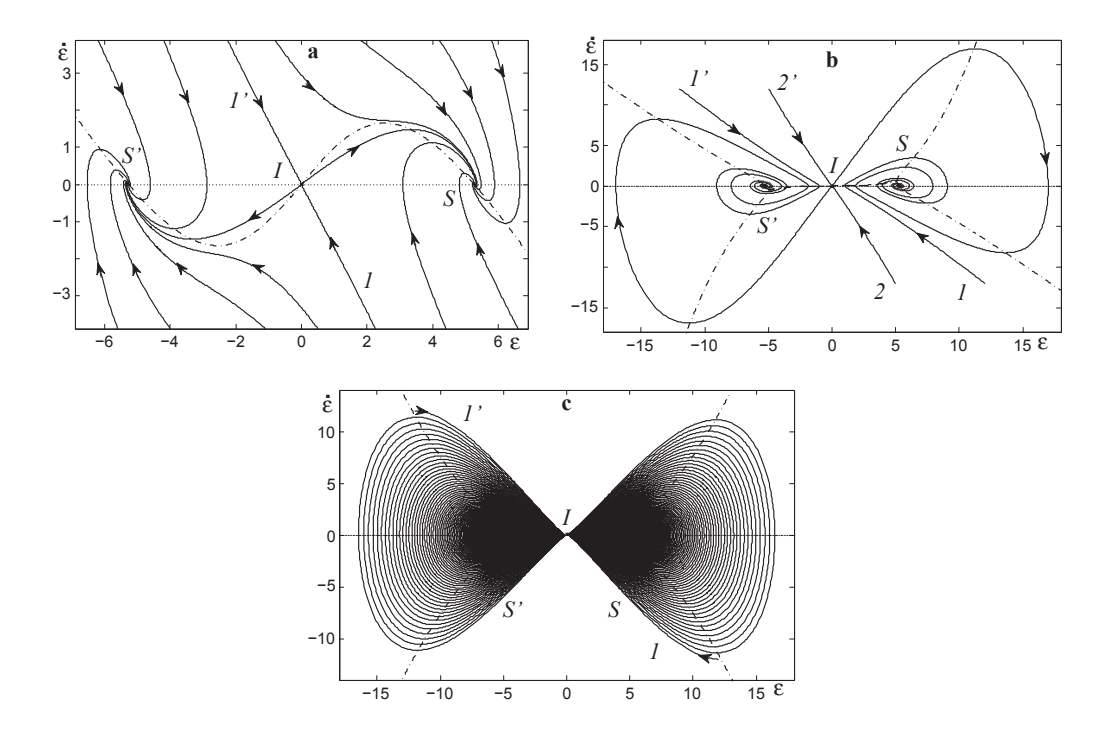


Figure 1: Phase portraits with parameters g=0.8 and  $T_e=30$  for noise intensity D=0, which are solution of (a) Eq. (6) for  $\tau=\tau_\sigma/\tau_\varepsilon=20$ ; (b) Eq. (13) for  $\tau=\tau_T/\tau_\varepsilon=100$ ; and (c) Eq. (15) for  $\tau=\tau_T/\tau_\sigma=100$ 

Figure 3a represents the solving the same equation as in the case of Fig. 2a but with low noise intensity  $D \neq 0$ . Therefore, the friction force fluctuates with small amplitude that meets the sliding mode at approximately constant velocity. The calculations are displayed from time t = 1000 because after this the stationary rubbing mode sets in.

The analysis of intensity  $S(\omega)$  of the signal in Fig. 3a indicates that the peaks are absent (figure 4a). Consequently, the time dependence F(t) is not characterized by the regular (periodic) components. It is apparent that this dependence on a double logarithmic scale indicates a downward trend with increase of the fluctuations frequency of the structural components in the This implies that fluctuations have a high energy at low frequencies Thus, it is obvious that the spectrum (power) of fluctuations of the  $\omega$ . evolutionary variables is inversely proportional to the frequency. Therefore, there are different time correlations in the system. This behavior is opposite to the properties of white noise, because in it the spectral density of the random signal assumes a constant value  $S(\omega) = const$  [25]. The spectrum decrease is due to the fact that in the initial equation (6) nonlinear terms, reflecting interactions of nonequilibrium state parameters (strains, stresses and temperature), serve as a filter that does not transmit high frequencies [10, 11, 26]. As a result, a transition occurs from white noise  $\xi(t)$ , inherent in most physical systems, to a colored one with a nonzero correlation time.

It is commonly recognized that many physical, biological and economic systems, which experience phase transitions, have stochastic (fluctuational) souse with power spectrum that is inversely proportional to the frequency. It is named  $1/\omega$ , flicker or less known as fractional (fractal) noise [27, 28, 29].

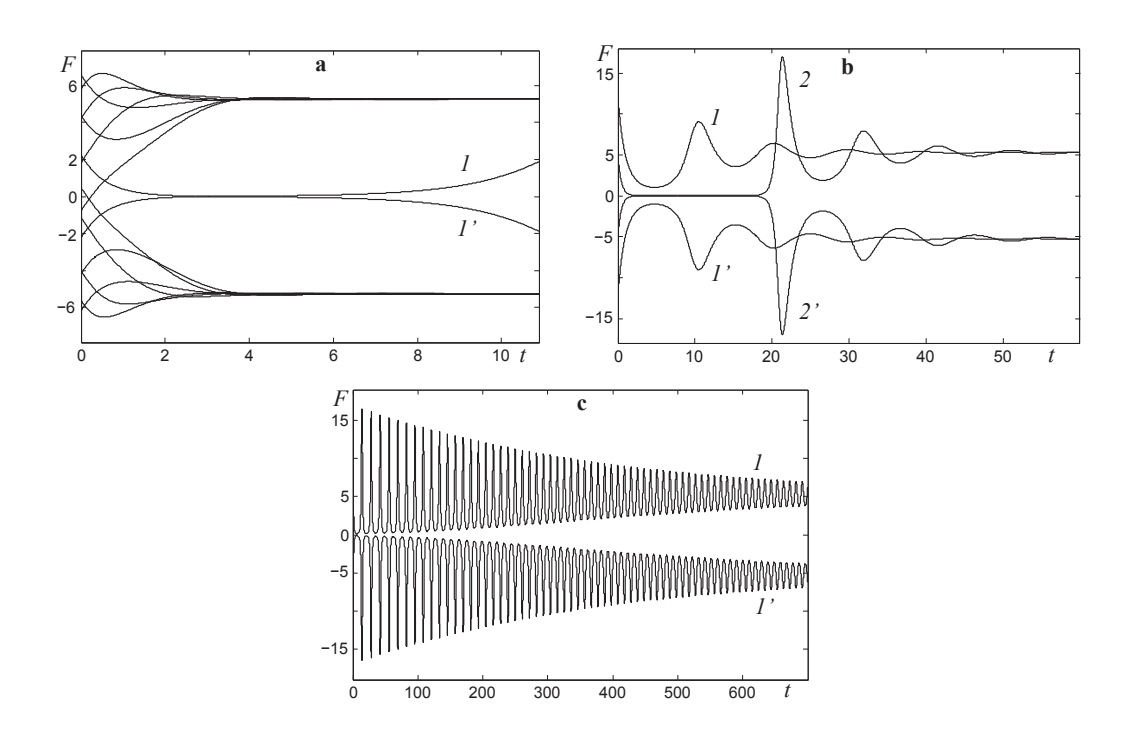


Figure 2: Time series of friction force F(t) corresponding to Fig. 1

In particular, similar activity takes place in many dynamical systems that undergo "white" noise and nonequilibrium transitions [27, 30, 31, 32]. Moreover, such pattern is observed during the various modes of plastic deformation [33, 34, 35, 36].

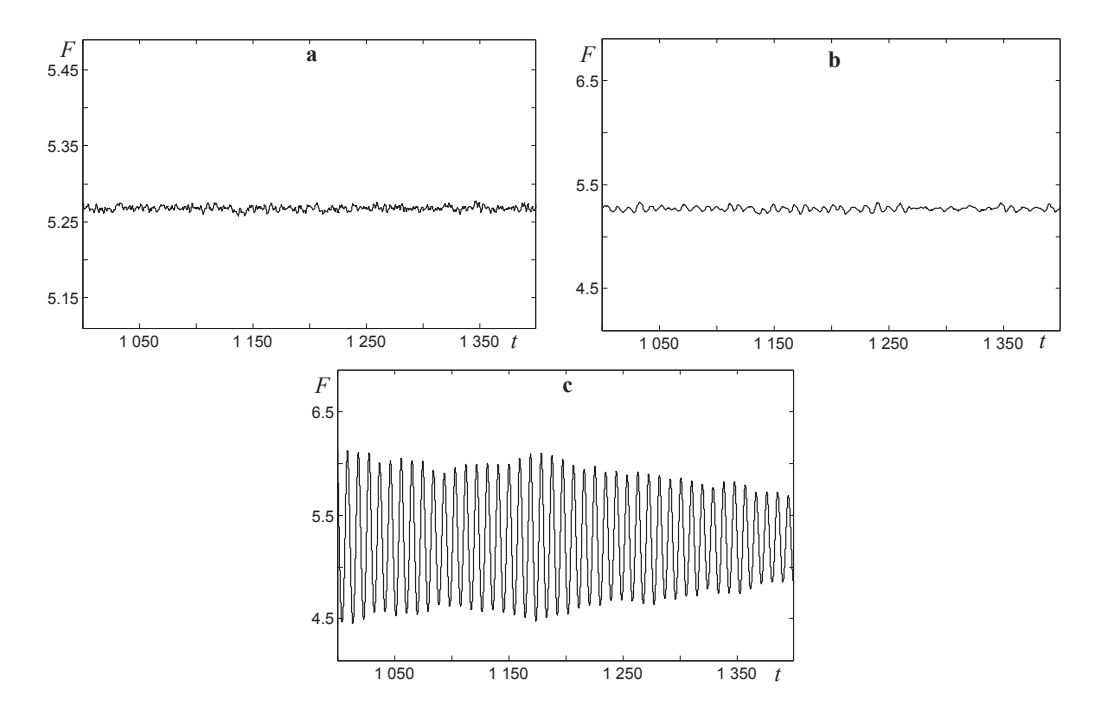


Figure 3: Time series of friction force F(t) corresponding to Figs. 1 and 2 for noise intensity  $D=5\cdot 10^{-5}$ 

The estimated values of relaxation slip time (Fig. 2a) and frequency of friction force fluctuations (Fig. 3a) allow to conclude that such behavior corresponds to the experimental dependencies of friction on displacement displayed in Fig. 3b in Ref. [2] and in Fig. 4c in Ref. [7]. Besides, stochastic and periodic F(t) are realized in experiments on rubbing of a polymer (poly(methyl methacrylate) PMMA), rubber and steel on ice [3, 4, 5] as well as on polycrystalline freshwater and saline ice over itself [2, 6, 7, 8, 9].

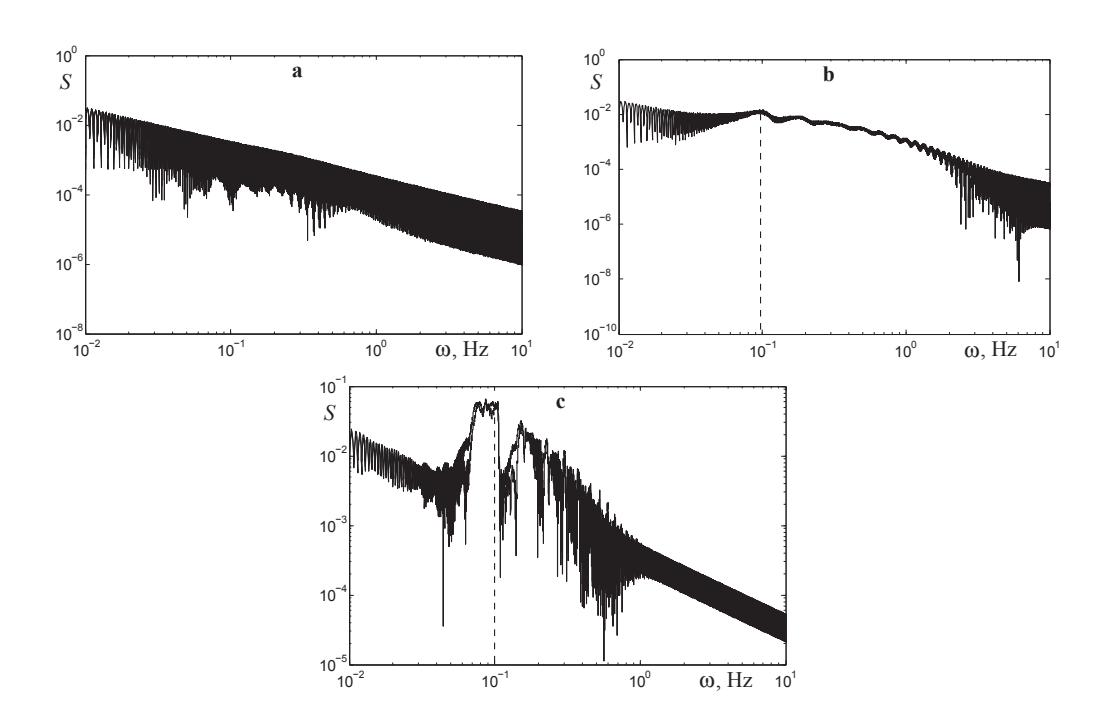


Figure 4: Spectral density of the signal  $S(\omega)$  corresponding to Fig. 3

## 2.2. The case $\tau_{\sigma} \ll \tau_{\varepsilon}, \tau_{T}$

As we did earlier, setting  $\tau_{\sigma}\dot{\sigma}\approx 0$  in the initial system we arrive at the equation

$$\ddot{\varepsilon} + \left[ \frac{1 + g\varepsilon^2}{\tau} - \frac{\dot{\varepsilon}}{\varepsilon} \right] \dot{\varepsilon} + \frac{\varepsilon}{\tau} \left[ 1 - g(T_e - 1 + \varepsilon^2) \right] = \xi(t), \tag{13}$$

where the time is measured in the units of  $\tau_{\varepsilon}$  and the ratio  $\tau = \tau_T/\tau_{\varepsilon}$  is introduced. Equation (13) fixes oscillations with the damping constant

$$\alpha = 0.5g\tau^{-1}(T_e - 1). \tag{14}$$

The phase portrait, that has been got by solving Eq. (13), is depicted in figure 1b. It is apparent that the same singular points are realized, the only difference lies in transformation of node points S and S' into stable focuses and more prolonged damping mode is observed. The numbers designate the phase trajectories in the figure. Contrary to the previous case the two isoclines appear, demonstrated by the dot-and-dash curves, owing to the dependence of damping constant on  $\dot{\varepsilon}$  in Eq. (13). The two-valued expression  $\dot{\varepsilon}(\varepsilon)$  for the isoclines  $\ddot{\varepsilon} = 0$  is obtained as a solution of a quadratic equation.

The rubbing force time dependencies (Fig. 2b) have long sections on which  $F \approx 0$  meeting the slow motion of friction surfaces. This implies that in the phase portrait the evolution of system occurs in the vicinity of origin  $(\varepsilon, \dot{\varepsilon} \approx 0)$  with a low rate of strain changing. However, a nonzero value of friction force appears always at sliding onset. The movement in two directions is not observed due to higher maximum of the effective potential at the coordinates origin.

The F(t) random series (Fig. 3b) describe a stationary mode with parameters that are not time dependent. To check the apparent periodicity

of this dependence the Fourier analysis is necessary. The  $S(\omega)$  spectrum in Fig. 4b displays the power weakening of signal with its frequency growth. But it is notable that at  $\omega \approx 0.1$  a maximum is realized showing the availability of a periodic component in F(t). Consequently, friction force changes periodically in accordance with Fig. 3b. Such behavior meets the oscillatory transitions between the crystalline and premelted ice resulting to the intermittent (stick-slip) mode.

Above the classification of the different states of ice is based on the following property. When shear strain  $\varepsilon = 0$  the ice is not premelted. The case  $\varepsilon \neq 0$  corresponds to its softening at ascent of thermostat temperature  $T_e > T_{c0}$  [10, 11, 12]. Expose this statement in more details. Let us assume that strains are initially small, that meets the crystalline ice as earlier. Beginning to move surfaces, we increase the values of  $\varepsilon$  according to any ascending section on the dependence depicted in Fig. 3b. At exceeding by strains the critical value softening occurs, then elastic component  $\varepsilon_{el}$  relaxes, and the total strains also diminish in accordance with the falling section of the curve. When due to relaxation the strains reach the values too low to preserve ice in the premelted state, the ice transforms in crystal, and the process reproduces itself. Thus, premelting takes place at large strains similar to above stated. It is worth noting that the scenario exposed in this subsection differs from that construed in previous subsection. Here, periodic transformations are observed between the crystalline and softened forms of ice, and stochastic variations of strains in them represent fluctuations that do not result to premelting/solidifing. Most probably that F(t) in Fig. 3b corresponds to experiments with freshwater, granular ice and columnar, saline ice [6] which

have disordered grain structure and are not characterized by strictly periodic friction force time series. Consequently, noises are laid on oscillations and the amplitude of the stick-slip transitions is not constant now. Besides, the fluctuations may result in instability of a focuses, i.e., continuous growth of the amplitude of friction force oscillations that resembles resonance. From estimations of relaxation time (Fig. 2b) and frequency as well as presence of periodicity of friction force oscillations (Fig. 3b) we can assume that such pattern meets the experimental data depicted in Fig. 3c in Ref. [2] and in Fig. 4b in Ref. [7].

## 2.3. The case $\tau_{\varepsilon} \ll \tau_{\sigma}, \tau_{T}$

By analogy with previous cases, let  $\tau_{\varepsilon}\dot{\varepsilon}\approx 0$ ; this yields equation

$$\ddot{\varepsilon} + \left[\frac{1}{\tau} - \frac{\dot{\varepsilon}}{\varepsilon}\right]\dot{\varepsilon} + \frac{\varepsilon}{\tau}\left[1 - g(T_e - 1 - \varepsilon^2)\right] = \xi(t),\tag{15}$$

where time is measured in the units of  $\tau_{\sigma}$  and  $\tau = \tau_T/\tau_{\sigma}$ . Now, the damping constant is fixed by the value

$$\alpha = 0.5\tau^{-1},\tag{16}$$

which, contrary to the previous subsections, depends only on factor  $\tau$  and descents with its increasing. From this it follows that the duration of oscillations ascents with growth of  $\tau$ , i.e., a larger number of oscillations occurs around the focus in Fig. 1c before the steady state sets in comparison to the above examined cases. This is confirmed by figure 2c demonstrating long-term oscillatory mode with negligibly low damping even during t=800. Figure 3c displays the driving fluctuational effect on the time dependence of

friction force that becomes more flat and regular comparatively with Fig. 3b (it is worth noting that noise intensity D is constant for all Figs. 3a–c).

Let us use the discrete Fourier transform for spectral analysis of friction force time series in Fig. 3c meeting the two phase trajectories in Fig. 1c. The corresponding spectrums (Fig. 4c) have a highest maximum at  $\omega \approx 0.1$ which are narrower than in Fig. 4b. Other maximums are more blurred, therefore the selected (significant) frequencies are equal to  $\omega \approx 0.1$ . At this frequency the 42 full oscillations are realized in the F(t) dependence in time interval  $\Delta t = 400$ . Thus, a more stable oscillatory intermittent mode with a larger amplitude establishes in this case of relationship between  $\tau_{\varepsilon}, \tau_{\sigma}, \tau_{T}$ . Namely, the conditions  $\tau_{\varepsilon} \ll \tau_{\sigma} \ll \tau_{T}$  expedite the appearance of periodic stick-slip ice friction. It is worth noting that for chosen parameters  $(g = 0.8 \text{ and } T_e = 30)$ , the steady-state value of dimensionless friction force  $F_0 \approx 5.2678 \; (AG_{\varepsilon} \; \text{is its measure unit}) \; \text{is reached with time in all examined}$ cases. It is apparent from Fig. 3 that fluctuations may result to nonessential stochasticity in the vicinity of the stationary value  $F_0$  (see Fig. 3a) or may influence on the behavior crucially, violating the rubbing mode (see Figs. 3b,c). From estimation of relaxation slip time (Fig. 2c) and form of rubbing force fluctuations (Fig. 3c) it follows that pattern examined in this subsection meets the experimental results depicted in Fig. 3d in Ref. [2] and in Fig. 4a in Ref. [7].

## 3. Conclusions

The above investigation shows that the viscoelastic model (1)–(3) with account of noise makes it possible to represent the main features of a stick-

slip mode of ice surface softening at friction. The kinetic pattern of these transitions is represented by the phase portraits shown in Fig. 1 and the time dependencies of friction force (Figs. 2 and 3). The type of singular point S corresponding to the softened ice depends on the relationship between relaxation times  $\tau_{\varepsilon}, \tau_{\sigma}, \tau_{T}$  of shear strain, stress, and temperature of ice surface. The above analysis shows that at absence of noise D=0 in the case  $\tau_T \ll \tau_{\varepsilon}, \tau_{\sigma}$  the point S is an attractive node, and after a short time interval the system reaches the stationary state (premelted ice). While at noise intensity  $D \neq 0$  intermittent mode represents diminutive fluctuations near steady-state value of friction force, probably, due to the rapid thermally activated processes. When the relationships between the relaxation times correspond to modes  $\tau_{\sigma} \ll \tau_{\varepsilon}, \tau_{T}$  and  $\tau_{\varepsilon} \ll \tau_{\sigma}, \tau_{T}$  at D = 0, the system undergoes more prolonged damped oscillations, i.e., point S transforms into focus. In the latter case noise leads to stick-slip regime with most expressed periodic component of rubbing force. A characteristic feature of this mode is that the relaxation time of temperature  $\tau_T$  is the greatest of the three.

## Declaration of competing interest

The authors declare that they have no known competing financial interests or personal relationships that could have appeared to influence the work reported in this paper.

#### Acknowledgements

The work was supported by the state project of Ukraine "Atomistic and nonlinear models of formation and friction of nanosystems" and visitor grant of Forschungszentrum-Jülich, Germany. A. K. is grateful to Dr. Bo N.J. Persson for hospitality during his stay in Forschungszentrum-Jülich.

## References

- [1] B. N. J. Persson, Ice friction: Role of non-uniform frictional heating and ice premelting, J. Chem. Phys. 143 (22) (2015) 224701, http://dx.doi.org/10.1063/1.4936299.
- [2] B. Lishman, P. R. Sammonds, D. L. Feltham, Critical slip and time dependence in sea ice friction, Cold Reg. Sci. Technol. 90-91 (2013) 9 13, http://dx.doi.org/https://doi.org/10.1016/j.coldregions.2013.03.004.
- [3] J. R. Blackford, G. Skouvaklis, M. Purser, V. Koutsos, Friction on ice: stick and slip, Faraday Discuss. 156 (2012) 243–254.
- [4] C. Klapproth, T. Kessel, K. Wiese, B. Wies, An advanced viscous model for rubber-ice-friction, Tribol. Int. 99 (2016) 169 181, http://dx.doi.org/http://dx.doi.org/10.1016/j.triboint.2015.09.012.
- |5| B. Marmo, J. R. Blackford, С. Ε. Jeffree, Ice fricand their dependence sliding veloction, wear features on ity and temperature, J. Glaciol. 51 (174) (2005)391–398, http://dx.doi.org/doi:10.3189/172756505781829304.
- [6] F. E. Kennedy, E. M. Schulson, D. E. Jones, The friction of ice on ice at low sliding velocities, Philos. Mag. A 80 (5) (2000) 1093–1110, http://dx.doi.org/http://dx.doi.org/10.1080/01418610008212103.

- [7] B. Lishman, P. Sammonds, D. Feltham, A. Wilchinsky, The rate- and state- dependence of sea ice friction, in: Proceedings of the 20th International Conference on Port and Ocean Engineering under Arctic Conditions, 2009, pp. POAC09–66.
- [8] E. Μ. Schulson, Α. L. Fortt, Friction of ice on J. ice, Solid (2012)Geophys. Res. Earth 117 (B12)B12204, http://dx.doi.org/10.1029/2012JB009219.
- S. [9] S. Sukhorukov, Friction of Loset, sea ice on Sci. Technol. 94 (2013)1 Cold Reg. 12, sea ice, http://dx.doi.org/http://dx.doi.org/10.1016/j.coldregions.2013.06.005.
- [10] A. Khomenko, Self-similar mode of ice surface softening during friction, Tribol. Lett. 66 (3) (2018) 82, http://dx.doi.org/10.1007/s11249-018-1034-x.
- [11] A. Khomenko, M. Khomenko, B. N. J. Persson, K. Khomenko, Noise effect on ice surface softening during friction, Tribol. Lett. 65 (2) (2017) 71, http://dx.doi.org/10.1007/s11249-017-0853-5.
- [12] A. V. Khomenko, K. P. Khomenko, V. V. Falko, Nonlinear model of ice surface softening during friction, Condens. Matter Phys. 19 (3) (2016) 33002, http://dx.doi.org/http://dx.doi.org/10.5488/CMP.19.33002.
- [13] O. Lahayne, B. Pichler, R. Reihsner, J. Eberhardsteiner, J. Suh, D. Kim, S. Nam, H. Paek, B. Lorenz, B. N. J. Persson, Rubber friction on ice: Experiments and modeling, Tribol. Lett. 62 (2) (2016) 1–19, http://dx.doi.org/10.1007/s11249-016-0665-z.

- [14] A. V. Khomenko, Y. A. Lyashenko, Periodic intermittent regime of a boundary flow, Tech. Phys. 55 (1) (2010) 26–32, http://dx.doi.org/10.1134/S1063784210010056.
- [15] A. V. Khomenko, I. A. Lyashenko, A stochastic model of stickslip boundary friction with account for the deformation effect of the shear modulus of the lubricant, J. Frict. Wear 31 (4) (2010) 308–316, http://dx.doi.org/10.3103/S1068366610040100.
- [16] A. V. Khomenko, N. V. Prodanov, B. N. J. Persson, Atomistic modelling of friction of Cu and Au nanoparticles adsorbed on graphene, Condens. Matter Phys. 16 (2013) 33401, http://www.icmp.lviv.ua/journal/zbirnyk.75/33401/art33401.pdf.
- [17] A. Khomenko, D. Troshchenko, L. Metlov, Thermodynamics and kinetics of solids fragmentation at severe plastic deformation, Condens. Matter Phys. 18 (2015) 33004, http://dx.doi.org/10.5488/CMP.18.33004.
- [18] L. Metlov, M. Myshlyaev, A. Khomenko, I. Lyashenko, A model of grain boundary sliding during deformation, Tech. Phys. Lett. 38 (2012) 972– 974, http://dx.doi.org/10.1134/S1063785012110107.
- [19] A. I. Olemskoi, A. V. Khomenko, Three-parameter kinetics of a phase transition, J. Exp. Theor. Phys. 83 (6) (1996) 1180–1192.
- [20] A. A. Andronov, A. A. Vitt, S. E. Khaikin, Theory of Oscillations, Nauka, Moscow, 1981, (in Russian); an earlier edition of this book was translated at Pergamon Press, Oxford (1966).

- [21] O. Mazur, L. Stefanovich, Pressure effect on the formation kinetics of ferroelectric domain structure under first order phase transitions, Physica D 424 (2021) 132942, https://doi.org/10.1016/j.physd.2021.132942.
- [22] O. I. Olemskoi, O. V. Yushchenko, T. I. Zhylenko, M. V. Prodanov, Study of quasi-equilibrium condensation kinetics using the phase plane method, Metallofiz. Noveishie Tekhnol. 32, No. 11 (2010) 1555–1569.
- [23] W. H. Press, S. A. Teukolsky, W. T. Vetterling, B. P. Flannery, Numerical Recipes: The Art of Scientific Computing, Cambridge University Press, New York, 2007.
- [24] A. V. Khomenko, O. V. Yushchenko, Solid-liquid transition of ultrathin lubricant film, Phys. Rev. E 68 (2003) 036110, http://dx.doi.org/10.1103/PhysRevE.68.036110.
- [25] H. Risken, The Fokker-Planck Equation. Methods of Solution and Applications, Springer-Verlag, Berlin, 1989.
- [26] A. Khomenko, D. Troshchenko, L. Metlov, Effect of stochastic processes on structure formation in nanocrystalline materials under severe plastic deformation, Phys. Rev. E 100 (2019) 022110, http://dx.doi.org/10.1103/PhysRevE.100.022110.
- [27] S. Kogan, Electronic Noise and Fluctuations in Solids, Cambridge University Press, 1996, http://dx.doi.org/10.1017/CBO9780511551666.
- [28] C. W. Gardiner, Stochastic Methods, 4th Edition, Springer-Verlag, Berlin, 2009.

- [29] I. V. Ovchinnikov, R. N. Schwartz, K. L. Wang, Topological supersymmetry breaking: The definition and stochastic generalization of chaos and the limit of applicability of statistics, Mod. Phys. Lett. B 30 (08) (2016) 1650086, http://dx.doi.org/10.1142/S021798491650086X.
- [30] K. Syamal, K. Prodyot, K. Jürgen, Complex Dynamics in Physiological Systems: From Heart to Brain, 1st Edition, Understanding Complex Systems, Springer Netherlands, Berlin, 2009, http://dx.doi.org/10.1007/978-1-4020-9143-8.
- [31] V. N. Skokov, V. P. Koverda, A. V. Reshetnikov, Self-organized criticality and 1/f fluctuation under conditions of nonequilibrium phase transitions, J. Exp. Theor. Phys. 92 (3) (2001) 535, http://dx.doi.org/10.1134/1.1364751.
- Structural of [32] A. Pogrebnjak, Α. Goncharov, features of formed coatings and films refractory compounds, Tekhnol. 38 Metallofiz. Noveishie (2016)1145-1166,http://dx.doi.org/https://10.15407/mfint.38.09.1145.
- [33] M. A. Lebyodkin, I. V. Shashkov, T. A. Lebedkina, K. Mathis, P. Dobron, F. Chmelik, Role of superposition of dislocation avalanches in the statistics of acoustic emission during plastic deformation, Phys. Rev. E 88 (2013) 042402, http://dx.doi.org/10.1103/PhysRevE.88.042402.
- [34] M. A. Lebyodkin, I. V. Shashkov, T. A. Lebedkina, V. S. Gornakov, Experimental investigation of the effect of thresholding on

- temporal statistics of avalanches, Phys. Rev. E 95 (2017) 032910, http://dx.doi.org/10.1103/PhysRevE.95.032910.
- [35] R. N. Mudrock, Μ. A. Lebyodkin, Р. Kurath, Α. J. Beaudoin, Τ. A. Lebedkina, Strain-rate fluctuations duruniform deformation ing macroscopically of a solutionstrengthened alloy, Scripta Mater. 65 (12) (2011) 1093 – 1096, http://dx.doi.org/https://doi.org/10.1016/j.scriptamat.2011.09.025.
- [36] A. V. Khomenko, M. V. Zakharov, K. P. Khomenko, Ya. V. Khyzhnya, P. E. Trofimenko, Atomistic modeling of friction force dependence on contact area of metallic nanoparticles on graphene, in: Proceedings of the IEEE 8th International Conference on Nanomaterials: Applications and Properties (NAP'18), IEEE, USA, 2019, Vol. 4, pp. 04NNLS15-1-4, https://doi.org/10.1109/NAP.2018.8915102.